Frontiers in Heat and Mass Transfer (FHMT), 20, 28 (2023)
DOI: 10.5098/hmt.20.28

Global Digital Central
ISSN: 2151-8629

Frontiers in Heat and Mass Transfer

Available at www.ThermalFluidsCentral.org

PERFORMANCE ANALYSIS OF AN ENERGY EFFICIENT PCM-BASED ROOM COOLING SYSTEM

Ummid I. Shaikh[a], Sonali Kale[b] Anirban Sur[c], Anindita Roy[c],

[a]*Department of Mechanical Engineering, Pimpri Chinchwad College of Engineering, Pune-411044, INDIA*
[b]*Department of Applied Sciences and Humanities, Pimpri Chinchwad College of Engineering, Pune-411044, INDIA*
[c]*Mechanical Engineering Department, Symbiosis Institute of Technology, Symbiosis International (Deemed) University, Pune, 412115, INDIA*

ABSTRACT

The requirement for sustainable development for buildings is to have environmentally friendly cooling and heating systems. The utilization of phase change materials (PCM) in the cooling system is a potential solution for minimizing active power requirements as well as for reducing the size of components of a vapor compression refrigeration VCR system. A prototype of an Air-PCM (T25™) heat exchanger was fabricated and tested in actual environmental conditions. Experimental trials using a salt hydrate as PCM have shown the maximum cooling effect of 2.05 kW when 75% of the PCM was solidified. Based on the results, it is found that PCM-based passive cooling has the potential to reduce the size (cooling capacity) of the air conditioner (AC) in the range of 13 to 46 %.

Keywords: *Free space cooling, Air-PCM heat exchanger, Numerical and experimental analysis*

1. INTRODUCTION

The issue of energy consumption and carbon dioxide emission in most countries arises mainly from buildings. The emission of greenhouse gases all the way through building air conditioners creates environmental issues. Therefore, it is necessary to move toward alternate solutions for environmental sustainability. The interest in the utilization of phase change material (PCM) in building envelopes is a growing concern to save energy and to get better indoor thermal comfort (De Gracia and Cabeza, 2015; Liu et al., 2018; Song et al., 2018; Turnpenny et al., 2000). The parametric study is important to achieve a better thermal performance of buildings encapsulated with PCM. In this regard, the parameters like PCM concentration (e.g., volume or mass), the impact of PCM location within the cavity of external walls, phase transition temperature and indoor and outdoor air temperatures are mainly considered. The numerical analysis is performed using a proven heat transfer model to analyze the thermal performance of a building wall with PCM (Ramakrishnan et al., 2016, Sun et al., 2022). It has been demonstrated that PCM-based cooling may be used to supplement the traditional vapor compression refrigeration (VCR)-based space cooling technology so as to minimize the power usage for air conditioning. A transient energy study using building envelopes filled with PCM (melting point of 24-26 ºC) was carried out by Khan et al., 2022. It is found that electricity consumption was lowered by 13.7 % in summer and 32.7 % in winter. Summer and winter power usage was lowered by 8.7 and 45.7 %, respectively with PCM (melting point of 28-30◦C). The researchers determined that PCM29 is superior in terms of lowering power usage. Bohórquez-Órdenes et al., 2021, recommended a method for optimizing the use of PCM in thermal housing to increase thermal comfort with reduced energy consumption in air conditioning (AC). Thermal discomforts were reduced from 14.29 % to 25.43 % using passive analysis and by 11% and 23% using active analysis. The monthly power bill was found to be lowered from 53 % to 71 %. The impact of PCMs on peak load shifting, peak temperature, and interior temperature variation was studied by Al-mudhafar et al., 2021 and simulation was also done using Ansys Fluent. PCM was used to reduce the interior air temperature. Furthermore, it was predicted that PCM with higher melting temperatures was proper for hot weather conditions. Ručevskis et al., 2020, built a PCM storage system with cold water capillary pipes in the ceiling slab and studied parameters such as PCM layer thickness, number of parallel pipes, pipe diameter, night cooling period, and cooling water intake temperature. A numerical simulation conducted under typical summer climatic conditions in the Baltic States revealed that the average interior temperature was reduced by 5 °C.

The PCM melting temperature of an office building in 15 locations across the world was optimized by utilizing simulation-based optimization and natural ventilation operation. In hot and dry environments, PCM-based free cooling was shown to be ineffective. However, in moderate conditions, the usefulness of PCM was raised from 3.32% to 25.62% by coupling a PCM passive system and further to 40% with temperature-controlled ventilation (Prabhakar et al., 2020). The effect of velocity and inlet air temperature on solidification and cooling performance was analyzed by Ratnakar Kulkarni, et al., 2015. In this study, encapsulated hydrated salt PCM (of melting point 29°C) in a double pipe heat exchanger with a copper inner tube was used. In the experimental observations, an average temperature drop of 0.8°C with inlet air at 34°C with 4m/s velocity was reported during day time. Reyes-Cubas and Abdo, 2020, used Ansys Fluent to simulate airflow in a two-dimensional chamber equipped with a wind catcher containing phase change materials (PCMs). In the room with PCM, the average temperature at 1.2 m high was reduced by roughly 1 to 2 °C compared to the room without PCM. Weinläder et al., 2016, observed the cooling effect in the ceiling of an energy center. In this work, salt hydrate PCM

Global Digital Central
ISSN: 2151-8629

was kept above and below the water pipes in the ceiling. Passive cooling power in between 10-15 W/m2 was estimated at operative room temperatures of 26°C by considering the specific heat load. A physical prototype of a latent heat storage unit was built and tested by Li et al., 2016. The average operational time of air conditioning was reduced by 17%, attributed to energy savings. Though a lot of work is reported on free space cooling using latent heat storage, relatively less literature is available on the study of PCM-based cooling under actual climatic conditions. Focus is laid on the integration of PCM in-room cooling applications and their thermal performance along with an innovative design of an air-PCM heat exchanger Also, there is limited research on the application of salt hydrates for space cooling, owing to their corrosive action on the metals like copper and aluminum which are preferred for encapsulation due to their high thermal conductivity. This work also provides a basis for more sophistication in the development of air-PCM heat exchangers for free space cooling applications.

To address this issue, this study reports experimental investigations on an Air-PCM (T25™) heat exchanger meant for free space cooling. Experimental as well as numerical investigation is carried out under actual environmental conditions in order to study the effect of various parameters on the melting and solidification behaviour of PCM. Night time cold air is routed through the heat exchanger for solidifying and the hot room air is circulated through the same heat exchanger for getting the cooling effect. Air inlet, outlet, and PCM temperatures are monitored in real-time during charging (Solidification) and discharging (Melting). The cooling effect in TR is calculated for various melting periods.

A schematic line diagram showing the operating principle of a PCM-based free space cooling system for buildings is shown in Figure 1. Its operation involves the charging and discharging of the thermal (PCM) storage unit. The charging process occurs during the night hours when the ambient temperature is relatively lower compared to room temperature. The cool ambient night air is allowed to flow through the thermal storage unit thereby removing heat from the liquid PCM which starts solidifying gradually. An electrically driven fan is used to circulate the air in the storage unit in order to reduce the solidification(charging) time. The charging process continues until the ambient temperature is lower than the melting/solidification temperature of PCM.

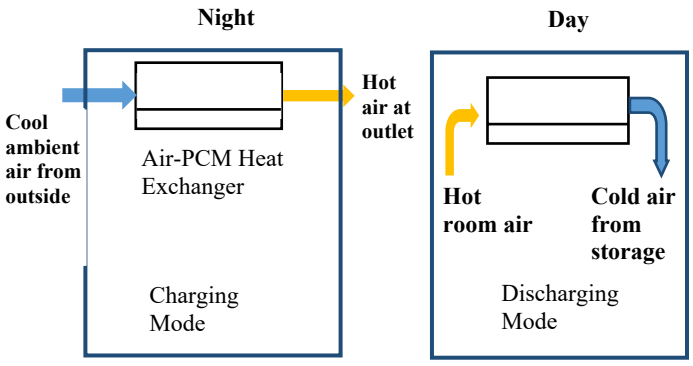

Fig. 1. Charging and Discharging process in free space cooling

The discharging mode of operation is initiated when the indoor temperature rises, i.e., during the daytime. The relatively hot room air is now allowed to be passed over the thermal storage unit allowing it to get cooled. Akin to a conventional air conditioning unit, the indoor air is cooled and distributed to the indoor room space, thereby catering to the heat load. In the discharging mode, the PCM absorbs heat from the room and air and undergoes a phase transformation from solid to liquid. This charging and discharging process continue with changes the ambient temperature. It is evident that such a cooling scheme is beneficial in regions that have a larger difference between their nighttime and daytime temperatures.

2. METHODOLOGY

In order to estimate the potential for free-space cooling using a phase change material, an experimental set-up comprising an air-PCM heat exchanger was built up. For building (room cooling) the experimental setup, the steps as depicted in Figure 2 were followed.

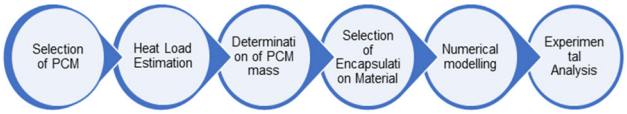

Fig. 2 Steps showing the execution of the study

Each of these steps is elaborately presented in the following sub-sections.

2.1 Selection of Phase Change Material

Paraffin and salt hydrate are commonly used PCM for free space cooling. A comparison of the characteristics of paraffins and salt hydrates was done to identify the best PCM for testing. Fsor the current study, salt hydrate is selected as it has a higher latent heat of fusion (150-300kJ/kg), a sharp melting point, relatively small volume variation, no fire hazards, and thermal stability (Mehling and Cabeza, 2008). The specifications of the PCM used for the experiment are as given in Table 1.

Table 1 Specifications of hydrated salt used as the phase change material

Parameter	*Value*
Product name	Latest^{TM}25T
Description	Viscous semi-solid near Phase Change Temperature
Appearance	Translucent
Base Material	Inorganic salt
Phase Material Temperature	24°C - 26°C
Sub-cooling	2°C max
Specific Gravity	1.48 – 1.5
Latent Heat Practically	175 Joules/g
Latent Heat Theoretically	188 Joules/g
Specific Heat	2 Joules/g°C
Thermal Conductivity	1Watt/m°C
Flammability	No
Thermal Stability	More than 10,000 cycles
Max. Operating Temperature	100°C

Free cooling of buildings coupled with PCM storage unit performs efficiently in the climatic conditions where the diurnal temperature range is between 12°C and 15°C (Medved and Arkar, 2008). According to the monthly average of maximum and minimum temperature data, the average diurnal temperature difference at the experiment site (Pune, Maharashtra State, India) is found to be 16 K (Table 2)

The melting point of PCM plays an important role in the design of the storage unit and should be chosen in such a way that it ensures maximum solidification during the charging process while keeping the air temperature within comfort levels during day time. Different

Global Digital Central
ISSN: 2151-8629

researchers proposed the different criteria, some of them are as given below:

(a) According to Medved and Arkar, 2008, the optimal melting temperature for free cooling application can be found from the following relation $T_m = T_a+2K$
(b) According to Lazaro et al., 2009, for free cooling applications, to maintain a specific temperature level when the cooling demand is high, the PCM phase chansge temperature should be lower. On the other hand, for very low cooling demand, the phase change temperature should be close to the objective temperature level.
(c) Another study suggests that cooling potential of the free cooling in dry and hot climatic conditions can be maximized by using PCM having melting point equal to the comfort temperature of the hottest summer month (Waqas & Kumar, 2011)

Considering the third criterion, the melting point of the PCM must be close to the designed room temperature. For comfortable human conditions, Design room temperature ~24 ºC (Arora, 2000). Therefore, for this study melting point of PCM is selected as 25 +/-1 ºC

Table 2 Daily Average Dry Bulb Temperature range for Pune (ISHRAE DataBook 2017)

Month	Max °C	Min °C	Range °C
Jan	31.5	12.9	18.6
Feb	33.6	11.8	21.8
Mar	38.4	14.6	23.8
Apr	39.4	18.9	20.5
May	41	20.5	20.5
Jun	39.3	22.6	16.7
Jul	31.5	22.8	8.7
Aug	29.6	21.4	8.2
Sep	30.7	21.4	9.3
Oct	33.2	20	13.2
Nov	31.2	13.4	17.8
Dec	29.8	12.8	17
Average	**34.1**	**17.8**	**16.3**

It is now imperative to estimate the quantity of PCM necessary to produce a specified cooling effect. This necessitates the estimation of the cooling load needed to be catered. The subsequent section deals with the heat load of a reference room which is conditioned by the said air-PCM heat exchanger.

2.2 Heat Load Estimation

The first step in designing any PCM-based system is to estimate the cooling load to be catered. In the present context, comfort air conditioning of a 150 sq ft apartment room is being considered. In order to maintain human comfort conditions, the components of heat load consist of (a) heat transmitted by the walls (b) heat transmitted by roof (c) heat transferred through fenestration (glass) (d) heat transferred due to infiltration during door openings (e) heat due to human occupancy (f) heat carried by ventilation air for maintain freshness as well as (g) heat generated due to the equipment present in the room. The components from (a) to (d) are categorized as external loads as they are dependent on the external weather conditions, while components (e) to (g) are internal loads. Table 3 lists input parameters used for the load calculation.

Heat load estimation consists of two components -external and internal. The procedure for estimation is detailed as under. The room considered here is part of an apartment with a sunlit west wall. This wall also contains a 1.5 mx1.5 m window. The external loads are estimated and detailed as under:

Table 3 Input parameters for heat load calculation (ISHRAE DataBook 2017)

Parameter	*Value*
Room Lx B x H	3m x 4.5 m x 4.5 m
Location	Pune, India 18.53 ºN 73.8 ºE
Inside conditions	27ºC dry bulb, 50%RH
Outside conditions	38ºC dry bulb, 24ºC Wet Bulb
Window on west wall	1.5 m x 1.5 m
U for wall	1.72 W/m^2.K
U for roof	1.14 W/m^2.K
U for floor	1.2 W/m^2.K
U for glass (double glazing, regular)	3.12 W/m^2.K
Solar Heat Gain (SHG) of glass	300 W/m^2
Internal Shading Coefficient (SC) of glass	0.80
Occupancy	75 W sensible heat/person and 75 W latent heat/person
Lighting load	12 W/m^2 of floor area
Appliance load	600 W (Sensible) 300 W(Latent)
Infiltration	2-4 Air Changes per Hour
Ventilation	2.5 lit/s/person
Factor of safety	25%

2.2.2External loads:

a) Heat transfer through the walls

Since only the west wall, which measures 3m x 4.5m and has a glass window of 1.5m x 1.5m, is visible, the rate of heat transfer through this wall is provided by Eq. (1). The term CLTD represents the cooling load temperature difference which accounts for the effective temperature difference accounting for both the steady state and transient heat transfer effects. From ISHRAE (ISHRAE DataBook 2017) for Group B type wall, the overall heat transfer coefficient is 1.72 W/m^2 K and CLTD is 17ºC. Rest of the other walls are not exposed to sunlight and hence do not contribute to the heat load of the room.

$$Q_w = U_w A_w CLTD_w \quad (1)$$

It may be noted that while calculating the heat gain through the wall, the area corresponding to the window should be subtracted. Using the above expression, the heat load of the room is determined as 329 W.

b) Heat transfer through roof:

The roof contributes sensible heat to the living space and is assumed to be constructed of 4-inch heavy concrete with 1" of insulation. The CLTD for the roof for 20 ºN latitude is 29.5 ºC and the overall heat loss coefficient (U_{roof}) is 1.14 W/m^2 K. Using Eq. (2), the heat gain by the roof is:

$$Q_{roof} = U_{roof} A_{roof} CLTD_{roof} \quad (2)$$

Accordingly, the heat load contributed by the roof is 454 W.

Global Digital Central
ISSN: 2151-8629

c) Heat transfer through glass
The window glass contributes to sensible heat gain by direct transmission of solar radiation. Quantity of heat transmitted is governed by the type of glass, presence of internal shading elements such as curtains, blinds etc., and the latitude of the place under consideration. The heat gain through glass consists of two components, one due to the combined convective and conductive heat transfer and the second due to the transmissivity of glass.

$$Q_{glass} = A_{glass}\,[\,U_{glass}(T_o - T_i) + SGHF.SC] \quad (3)$$

The second term in equation (3) is the transmission heat gain and is determined using the solar heat gain factor (SGHF), while the shading effect of curtains is taken into account by the parameter shading coefficient (SC). Using the values listed in Table 2, the heat gain through glass is 657.72 W/m^2.

c) *Heat transfer due to infiltration*
Outside air enters the room when doors or windows are opened, thus contributing to infiltration heat load. Since air entering the conditioned space comprises of moisture, it contributes to both sensible and latent heat load on the air conditioning device. Infiltration is usually determined from the number of air changes per hour (ACH) which accounts for the number of times air equivalent to the volume of the conditioned space (room) enters in time duration of 1 hour. It is estimated as follows:

$$Q_{inf,s} = V_{inf}\rho\, c_{pa}(T_o - T_i) \quad (4)$$
$$Q_{inf,l} = V_{inf}\rho\, H_{fg}(\omega_o - \omega_i) \quad (5)$$

where C_{pa} is specific heat of air at constant pressure, ρ_a represents the outdoor air density, T_i is the room air temperature, T_o is outdoor air temperature, ω_i is specific humidity of room air, ω_o is the specific humidity of outdoor air while H_{fg} represents the latent heat of evaporation of water in kJ/kg. For a residential apartment, the ACH is taken as 2. Accordingly, the infiltration heat load is 280 W (sensible) and 50W (latent).

Having estimated the external heat loads, it is now sought to determine the internal heat gains from the conditioned space.

2.2.3 Internal heat gains:

The internal heat gains are attributed to the following components:

a) Load due to occupants
Occupants in the conditioned space add both sensible and latent heat components. While, sensible heat is a function of the activity level of the occupants (metabolic rate), the latent heat component is contributed by respiration. Larger number of occupants raises the internal heat load. Cooling load due to occupants is estimated as-

$$Q_{s,occ} = Ox\; Q_{sensible/person} \quad (6)$$
$$Q_{l,occ} = Ox\; Q_{latent/person} \quad (7)$$

Where *O* represents the number of occupants in the room. In this study, the maximum number of occupants are considered as 4. Accordingly, the sensible and latent heat load per person is estimated considering seated light work which is typical to hotels/apartment rooms.

b) Load due to lighting
Since lighting involves both radiative and convective heat transfer, it adds sensible heat to the living space. The design lighting for apartment rooms range from 0.75 to 1.11 W / ft^2 (ISHRAE DataBook 2017). Hence, for the present case, the sensible heat due to lighting is 1.11x150 = 166. 5 W.

c) Load due to appliances
Appliances utilized in the conditioned space increase the latent and sensible loads. The sensible load may be in the form of radiation and/or convection. Since, the present study is restricted to residential use; it is not likely to have high-power appliances. It is assumed that small equipment such as hair dryers, coffee makers present in the room may add a sensible load of about 600 W and latent heat load of about 400 W.

Load due to ventilation is neglected in the present study. However, a factor of safety of 1.25 is assumed for any unforeseen loads which may raise the heat load of the space. Using the above heat load calculation, the total heat load is estimated given in Table 4.

Table 4 Breakup of the total load contributed by the room

Load Type	*Sensible, W*	*Latent , W*
External		
Walls	329	-
Roof	454	-
Glass	657.7	
Infiltration	280	50
Internal		
Occupants (4 nos)	300	300
Lighting	166.5	
Appliance	600	400
Total	2787.2	750
Grand total	3537 x 1.25 = 4.42 kW_{th}	

From Table 3, the grand total cooling load is 1.25 TR and the sensible heat factor of the room is 0.86. It is now imperative to estimate the quantity of PCM required to serve the above calculated heating load.

2.3 Determination of PCM mass

The mass of PCM required can be estimated from the total heat load of the conditioned space and the latent heat capacity of the PCM. This heat is absorbed by the frozen PCM which causes a change in phase to a liquid state. As this heat would lead to a phase change of the material, the mass of the PCM required can be determined from the latent heat (L) and the heat load on the PCM in time duration of 1 hour is

$$m = \frac{Q_{tot}}{L} \quad (8)$$

From Eq. (8), the mass of the PCM is estimated to be 29 kg. It may be noted that the above estimation does not account for inefficiencies associated with the charging and discharging process.
In order to provide a proper heat exchange surface, the PCM is required to be encapsulated effectively. This necessitates the design of the containment which would allow for quick transfer of heat and is discussed in detail in the subsequent section.

2.4. Material Selection for Encapsulation

For space cooling applications PCM is encapsulated in concrete, gypsum wallboards, ceilings and floors (Iten et al., 2016). Concrete blocks or bricks are also used to encase PCM for space cooling applications (Castell et al., 2010). When used in heat exchanges, PCM is also filled in tubes of copper or aluminum for better heat conduction. In this work used plastic bags are utilized for encapsulating the PCM material due to ease of availability, non-corrosive nature, lightweight, and low cost. Metals such as copper and aluminium are not considered despite their high thermal conductivities since salt hydrates are corrosive to these metals (Moreno et al., 2014). Thin plastic sheet is used for encapsulating the PCM material due to its ease of availability, non-corrosive nature, lightweight and low cost. An initial trial was conducted using plastic bags with a thickness of 25 microns and 50 microns. The plastic bags

Global Digital Central
ISSN: 2151-8629

contained PCM and were clamped to a supporting framework. For quick solidification of the PCM, cold air was blown across it for two hours with a table fan. This procedure was repeated for two different thicknesses of plastic bags. Plastic bag of 25 microns was selected for PCM encapsulation as it was observed that the PCM gets solidified completely in the given period. It was also found that the PCM bag could bear a weight of 0.5 kg without sagging and with complete PCM solidification. Total amount of 30kg of PCM was available. As a result, the number of plastic bags required would be 60.

In order to verify and provide a confidence in the experimental results, a numerical modeling of the proposed set up was carried out. This is presented in the succeeding section.

2.5 Numerical Modelling to estimate PCM temperature

The PCM model's schematic is displayed in Figure 3. It is made up of several PCM stag layers. Layers are arranged parallel to one another. Each layer divided into two pouch and layers are placed parallel to each other. Room air flows through the gap between two layers. Hot room air moves between the cold PCM layers during discharging, at daytime. The PCM pouch's first outer wall warms up with hot air. Here, heat is transported inside the PCM pouch through convection so the temperature of solid PCM wall goes increase. The temperature of the PCM inside the pouch rises after that through conduction and starts melting after reaching its melting point

The heat from the PCM is removed at night by the movement of cool air inside the layers of the PCM. In this instance as well, the PCM boundary wall temperature begins to freeze when the PCM outer temperature hits its freezing point. The PCM boundary nodes are where freezing begins, and from there it moves to the inside nodes. The temperature difference between the room air passing through the PCM layers passage and the PCM wall is initially large, but it eventually decreases when thermal equilibrium is reached, which l also slow down the rate of heat transfer.

Here, there is a horizontal and vertical heat transfer between the PCM and room air. The temperature differential between the axial temperature of the room air and the temperature variation on the PCM wall causes heat transfer in the horizontal direction (axially). However, due to the model's simplicity, horizontal heat flow has been disregarded, and it is assumed that the temperature along the PCM border and the horizontal air flow are both constant. Therefore, in this instance, heat only moves vertically between the PCM layers and the room airflow. The following assumptions when developing the PCM numerical model.

i. Air between two PCM slabs flows in and has a constant temperature and viscosity.
ii. The impact of relative and specific humidity on the air in a room is neglected.
iii. Convective heat transfer resulting from natural airflow was likewise omitted, with the exception of the area of the PCM slab (vertical direction), where the PCM slab has restricted airflow.
iv. PCM thermophysical properties only depend on the solid or liquid phase and are temperature independent.
v. The entire PCM slab (control volume) is homogeneous and isotropic.

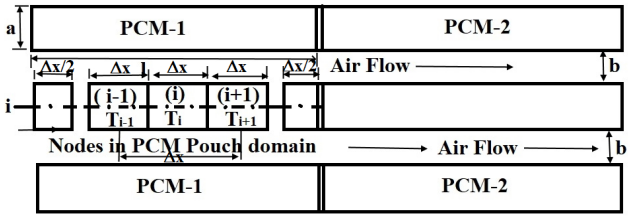

Fig. 3. Detail modeling of PCM layers

Numerical model for PCM slab is based on enthalpy model. Enthalpy (H) of PCM slab is denoted by equation 1 where sensible heat (q J/kg) and latent heat of fusion (L J/kg) and solid / liquid melting fraction (f) are included.

$$H = q + Lf_i \tag{9}$$

Total sensible heat of PCM calculated by the help of Eq.10 where solid PCM temperature increases from initial temperature (T_i) to solid to liquid melting temperature (T_m). c represents the specific heat of melting temperature (J/kg ^oC)

$$q = \int_{T_m}^{T_i} c\, dT \tag{10}$$

Solid/ Liquid fraction (f_i) varies 0 to 1. 0 is for solid when temperature of PCM less than T_m and 1 is for liquid when PCM temperature greater than T_m. Solid/ Liquid fraction f_i is also dependent on time. Total enthalpy (H) should be transferred to the PCM through conduction only. Then energy equation can be written as

$$H = \frac{k}{\rho}\left(\frac{\partial^2 T}{\partial x^2}\right) \tag{11}$$

where right hand Eq. 11 denotes 1D transient conductive heat equation for constant thermal conductivity, specific heat and density of PCM. After substituting Eq.11 in Eq.9, it becomes:

$$c\,\frac{\partial T}{\partial t} + L\frac{\partial f_i}{\partial t} = \frac{k}{\rho}\left(\frac{\partial^2 T}{\partial x^2}\right) \tag{12}$$

Here, a single slab has been split into two identical pieces. For the sake of creating a mathematical model, we are simply studying one component and treating it as symmetrical on both the left and right dividers. The entire domain of the rectangular PCM section (Fig. 3) has been partitioned into N evenly spaced nodes. Each node has an x-thickness and a control volume (CV). Initial and end node are contained half thickness $\left(\frac{\Delta x}{2}\right)$.By applying discretization and backward differential method on a single node i, and when the PCM is in total solid or liquid phase (f_i = 0 or 1) latent heat terms vanishes and Eq. 12 can be written as :

$$c\,\left(\frac{T_i - T_i^{n-1}}{\Delta t}\right) = \frac{k}{\rho \Delta x^2}(T_{i-1} - 2T_i + T_{i+1}) \tag{13}$$

From above equation T_i^{n-1} can be calculated as

$$T_i^{n-1} = \left(\frac{k\Delta t}{\rho c \Delta x^2}\right)T_{i-1} + \left[1 + 2\left(\frac{k\Delta t}{\rho c \Delta x^2}\right)T_i - \left(\frac{k\Delta t}{\rho c \Delta x^2}\right)T_{i+1}\right] \tag{14}$$

When PCM is in melting or solidification condition (f_i is in 0 to 1) there is no change in sensible heat so $c\,\frac{\partial T}{\partial t}$ in Eq. 12 becomes zero. Hence, for isothermal phase change condition of PCM, solid to liquid fraction (f_{li}) can be calculated from Eq. 12

$$L\frac{\partial f_i}{\partial t} = \frac{k}{\rho}\left(\frac{\partial^2 T}{\partial x^2}\right) \tag{15}$$

$$f_{li} = \frac{k\Delta t}{\rho L \Delta x^2}(T_{i-1} - 2T_i + T_{i+1}) \tag{16}$$

Eq. 16 aids to determine the liquid fraction value on all nodes of the PCM pouch shown in Fig 3. Equations (14-16) have to be solved by applying heat transfer boundary conditions. Initial boundary conditions of PCM are that at x =0 and t =0 temperature of PCM = T_o (initial temperature). If convected heat from air to PCM interface is conducted to PCM body,

Global Digital Central
ISSN: 2151-8629

then the governing energy equation can be written using Fig 3 thermal circuit (Fig4) we can write:

$$-kA\,\frac{\partial T}{\partial x}|_{x=o} = hA_p[T_a(t) - T(0,t)] \quad (17)$$

$$-k\,\frac{\partial T}{\partial x}|_{x=l} = h\,[T(x,t) - T_a(t)] \quad (18)$$

where $T_a(t)$ is the air temperature which passes between the two PCM layers, $T(0,t)$ and $T(x,t)$ are PCM pouch surface temperatures.

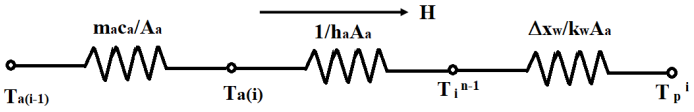

Fig. 4 Thermal circuit for air to PCM pouch heat transfer

For the air passage cross section area (A_a) at any distance x from the inlet heat transfer equation can be written by the help of the thermal circuit.

$$m_a.c_a\frac{dt}{dx} = h_a P_a\,(T_w - T_{ax}) \quad (19)$$

Where m_a is the mass flow rate of air which can be calculated as

$$m_a = V_a \times A_a \times \rho_a \quad (20)$$

Where ρ_a is the density of the air (kg/m^3) and V_a is the velocity of air (m/sec), h_a is the convective heat transfer coefficient of air flow (W/m^2°C) and P_a is the wetted perimeter between PCM wall and the air flow. For finding h_a, the following co-relation was used

$$Nu = 0.664 \times Re^{0.5} \times Pr^{0.33.} \quad (21)$$

Solution to the numerical model described in this section was used to obtain the temperature of the PCM. These results are compared to the experimental results and are detailed in section 4.

3. DETAILS OF EXPERIMENTAL SET UP

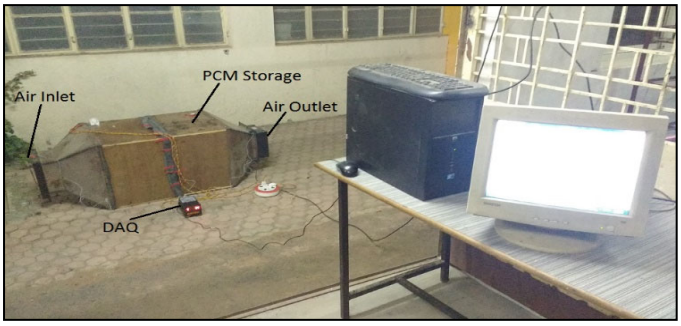

Fig. 5(a) Experimental setup for the air-PCM Heat Exchanger

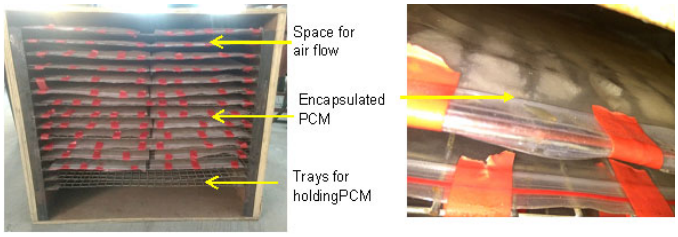

Fig. 5(b) Cross-sectional view of the heat exchange arrangement

The actual experimental set up is shown in Figure 5. The PCM storage is designed such that one plastic bag can slide in one plane as shown in Fig. 5 (b). Two such units are kept in series. The material to be used for the fabrication of this structure is wood as it provides insulating effect and non-corrosive property.

The schematic line diagram of the experimental set up developed is as shown in Figure 6.

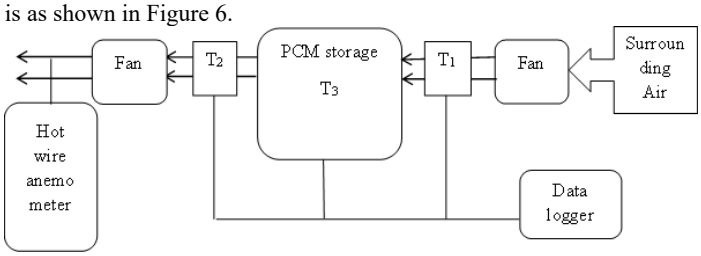

Fig. 6. Schematic diagram of experimental setup

Here, T_1 is the inlet temperature of air, T_2 is the outlet temperature of air,T_3 is the temperature of PCM. The PCM storage unit consists of a wooden cabinet and wire mesh trays for holding the PCM bags (Fig 5(b)). Each storage unit has an outer wooden cabinet and 15 wire mesh trays fitted in it. Two such storage units are kept in series. PCM filled bags are placed on the wire mesh trays and the storage unit is closed with rubber gasket to seal the gap and avoid leakages. The draft tubes are attached at both the ends of the storage unit for entry and exit of air. Two RTD sensors (resolution 0.1°C) are mounted at the entry and exit of the air. Another RTD sensor is placed in a PCM filled bag to measure the temperature of the phase change material. All the RTDs are connected to 8-channel data logger (TC-800D with accuracy0.25% of F.S.) which continuously measures the temperatures at specific interval of time. Two fans (each of 65 W) are mounted, one at inlet to draw atmospheric air in to the PCM unit and the other at outlet for creating additional suction. Hot wire anemometer (velocity range of 0.2 - 20.0 m/s, with accuracy of ± (1% + 1d) full scale), is used to measure the velocity of supplied air.

3.1. Experimental Investigations

Experimental investigations were carried out under actual climatic conditions in the month of April, which is midsummer in India. During these experiments, the solidification of the PCM happens at night and melting during the day. This section details the procedure of the charging (solidification) and discharging (melting) cycles undergone by the PCM. The parameters measured were T_1 (inlet temperature of air), T_2 (outlet temperature of air) and T_3 (temperature of PCM), air velocity and solidification time. Real time temperatures data was captured by the DAQ at the interval of 10 min.

3.1.1 Charging Test

Experimentation for solidification is carried out in night time. During this, night time air from outside is allowed to flow through the PCM storage unit. A fan is used to force the air over the PCM at relatively high velocity. Stepwise procedure for the charging test is elaborated as follows:

1. From visual inspection, ensure that entire PCM is in the liquid phase
2. Close both the ends of the air-PCM heat exchanger and
3. Switch on the fan and select appropriate velocity of the air
4. Switch on the data logger and record the inlet and outlet air temperature as well as the PCM surface temperature for every 10 minutes
5. Stop the test when either the entire PCM mass has solidified or the ambient temperature is greater than the melting point of the PCM.

Global Digital Central
ISSN: 2151-8629

3.1.2 Discharging Test

During the day, hot air from the room is circulated through the PCM unit at a velocity of 4m/s, which corresponds to human comfort levels. The PCM absorbs latent heat from the environment thereby cooling the room air. Melting hours were calculated from the measurements. Procedure for the discharge test is elaborated as follows:

1. From visual inspection, note the percentage of PCM solidified.
2. Close both the ends of the air-PCM heat exchanger unit.
3. Set the motor speed and accordingly adjust the air velocity so as to get a reasonable difference between the inlet and outlet air temperatures.
4. Switch on the data logger and record the inlet and outlet air temperature as well as the PCM surface temperature for every 10 minutes
5. Stop the test when either the entire PCM mass has melted or the PCM surface temperature exceeds 30 ºC.

Drop in the temperature of the room air and cooling effect in TR are calculated from the recorded data as shown below. The cooling effect of the PCM-heat exchanger is estimated from the rate of heat transfer (Q_{PCM}) from the PCM to the air using equation (22)

$$Q_{PCM} = \dot{m}C_p(T_{in,avg} - T_{out,avg}) \quad (22)$$

Here, $\dot{m}$ is the mass flow rate of air in kg/s and C_p is the specific heat air at constant pressure. The mass flow rate is calculated using Eq.(23)

$$\dot{m} = \rho AV \quad (23)$$

Where, ρ is the density of air at the said temperature, A is the flow area and V being the velocity of air. Density of air is calculated using ideal gas relation, where p is the pressure, R is the gas constant and $T_{in,avg}$is the average inlet temperature.

$$\rho = \frac{p}{R\,T_{in,avg}} \quad (24)$$

In order to gauge the potential of a free space cooling system to cater the heat load of a residential apartment, the percentage reduction in the size (capacity) of an air conditioner is calculated. This is done by considering a requirement of 1.25 TR for a room of 150 ft^2 as estimated in the heat load calculation of Section 2. As a base case, the load is assumed to be met by vapour compression refrigeration (VCR) run air conditioner. Accordingly, the percentage reduction in AC capacity is estimated as follows:

$$\%Reduction\ in\ AC\ capacity = \frac{Q_{VCR} - Q_{PCM}}{Q_{VCR}} \quad (25)$$

The terms Q_{VCR} indicates the rated capacity catered by a VCR run air conditioner, while the heat load supplied by the PCM heat exchanger is Q_{PCM}. A 100 % reduction in capacity would indicate that the PCM heat exchanger can entirely substitute a conventional air conditioner.

4. RESULTS AND DISCUSSION

Salt hydrates with melting point 25ºC (Latest^{TM}25T) PCM was used for experimentation. The experimentation was carried out in actual climatic conditions for solidification and melting. These are presented in the following sub-sections.

4.1. Results of charging of PCM

Figure 7 shows the temperature variation of PCM, inlet air and outlet air with time during charging when air velocity was 17m/s, while Figure 8 illustrates climate variables such as global solar radiation and ambient temperature recorded during a typical day of May at Pune 18.5° N, 73.8° E in the test period. A diurnal temperature difference of 13 °C is noted from Figure 8. The month of May has typically clear sky conditions which manifest in a smooth solar radiation availability during this period. The tests were conducted from about 12:00 am midnight and continued for about 7 to 8 hours (~450 minutes) till the morning about 6 am. After this, charging was not possible as surrounding air temperature would rise. Temporal variation of inlet and outlet air as well as PCM temperature are shown in Figure 7. It is noted from the graph that solidification has started after about 100 minutes and continued up to 350 minutes, after which the temperature of PCM remained constant. Thus, it can be concluded that complete solidification took about 6 hours minutes. The inlet air temperature varied from 25ºC to 22ºC. The average air inlet temperature was found to be 23ºC. Visual inspection indicated that about 25% of the PCM was solidified.

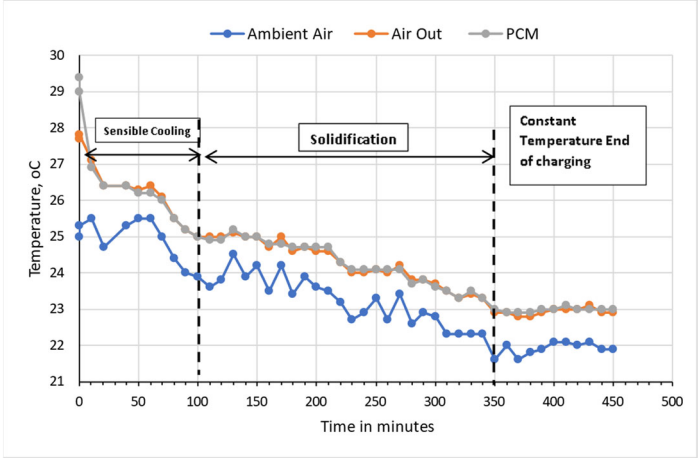

Fig. 7 AirTemperature variation with time during charging for velocity 17m/s

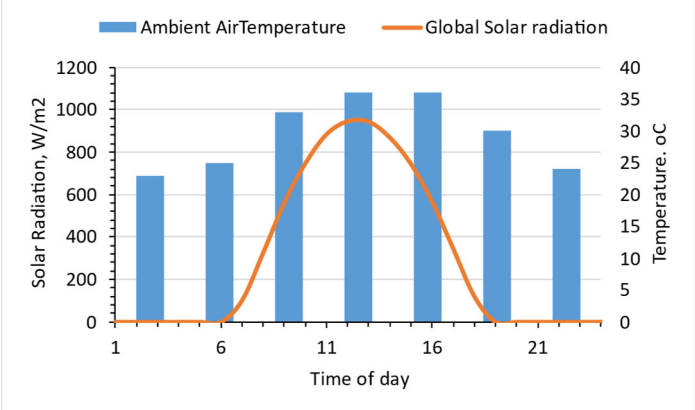

Fig. 8. Record of solar radiation and temperature on 10th of May at Pune, India

4.2 Results of discharging test

In order to study the effectiveness of the said free space cooling scheme, the PCM which was charged overnight is discharged in the morning. Details of four numbers of discharge tests are presented as detailed in Table 2. During each of these tests, the fraction of PCM solidified varied from about 25 to 75 % leading to variation in the outlet air temperature and the duration of discharge. The melted fraction was determined based on visual observation. The discharge was terminated when the inlet PCM surface temperature was greater than 30ºC, which ensured that the entire PCM was melted. Inlet and outlet air temperatures were recorded during the entire test period with an interval of 10 to 15 minutes. It may be noted that though the PCM mass selected was designed for catering a 1-hour cooling load duration, the actual discharge duration (Table 2) is much larger. This is attributed to the efficiencies in the charging and discharging process and inlet air temperature which is climate dependent.

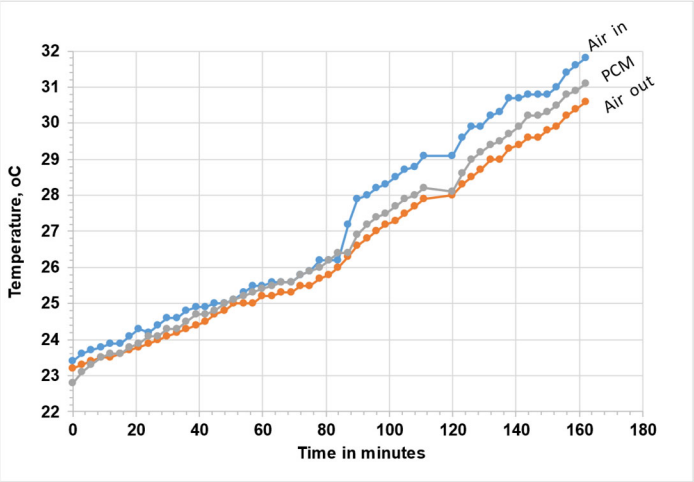

Fig. 8 Air temperature profile during discharging from 40% solidified state during Test no. 2

Figure 8 illustrates the chronological record of PCM, inlet air and outlet air temperature with time during discharging when air velocity was maintained at 6 m/s. The inlet air temperature (T_{in}) varies from 23.5°C to 32°C over about two hours and sixty minutes of the testing period. The average air inlet temperature, $(T_{in})_{avg}$was found to be 27.1°C. The outlet air temperature (T_{out}) varied from 23°C to 31°C. The average air outlet temperature $(T_{out})_{avg}$ during the test period was found to be 26.4°C. The average temperature drop observed was 0.7°C.

4.3. Experimental vs. numerical simulation result

Using the Gausses-Seidel iterative approach and Python code, the equations 9 to 21 have been solved to determine the temperatures at various nodes and the surface temperature of the PCM pouch illustrated in Figure 9. In order to solve heat, transfer via the air on the following iteration, the temperature at various nodes and the surface temperatures derived from the PCM mathematical model are used.

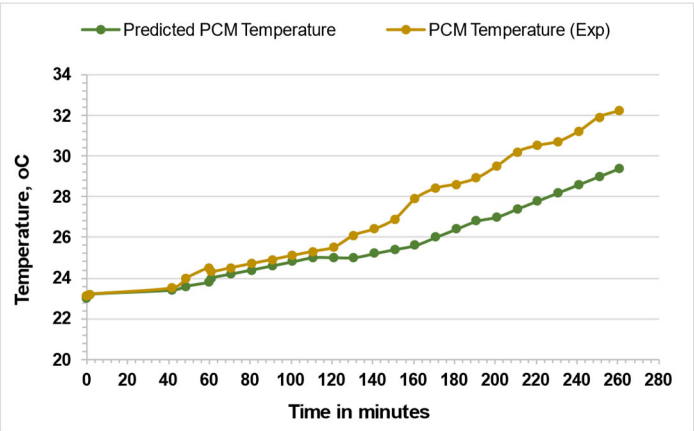

Fig. 9 Results of numerical modelling showing chronology of actual vs predicted PCM temperature.

Fig. 3 is the schematic of the PCM slabs and actual diagram is shown by Fig 5b. The PCM storage (Fig. 5b) is made up of a number of parallel layers of PCM slabs. The spaces between the PCM slabs are ventilated. Adopting the "constant heat flow" or "constant temperature" case for this model is unsuitable because the temperature of the air entering the PCM storage can be either constant or fluctuating. Figure 9 shows the predicted temperature of the PCM using the above numerical modelling technique. It is seen that initially up to 120 minutes, the difference between the experimentally measured and predicted temperature is of the order of 1%. However, later, the error gradually keeps on rising. In reality, air also contains additional gases like CO_2, NO_2, and others. But we took the idle condition into account in the mathematical model. The air outlet temperature is higher than predicted by the numerical model due to the presence of CO_2 more than the ideal condition. The average error is 4.7% which is reasonable.

4.4. Reduction in AC capacity

Table 5 summarizes the observation and results of the calculations during discharging (melting) process for different melting durations. Experimentation is carried out in the month of May, which registers the highest temperatures in summer in the Indian subcontinent.

Table 5 Results of discharging process

Test no.	Average inlet air temperature (°C)	Fraction of PCM solidified during night hours	Cooling Effect Q_{PCM} (kW_{th})	Average temperature drop (°C)	Maximum tempera-ture drop (°C)	% Reduction in AC capacity
1	25.5 °C	25 %	0.6	0.41	0.8	13.6
2	26.7 °C	40 %	1.02	0.7	1.5	23.1
3	27 °C	50 %	1.16	0.8	1.5	26.5
4	27.6 °C	75%	2.04	1.4	1.7	46.3

The cooling effect is calculated for a discharge velocity of 4 m/s, an area of the heat exchanger of 0.3 m^2 (0.58 m x0.52 m), and C_p of air as 1.005 kJ/kg K. Following the procedure detailed in section 3, the cooling effect during each of the discharge test was estimated and are presented as given in Table 4. The discharge was observed to take place in a time duration of 2 to 3 hours during tests 1 to 4. The fraction of PCM solidified at the beginning of the discharge varied from 25 to 75 % as recorded from visual observation. Accordingly, a temperature drop in the range of 0.5 to 1.5 °C was observed. It may be noted that as the temperature drop is relatively low, it is necessary to have relatively high air velocity to ensure thermal comfort. The size reduction of the AC in the range of 14 to 46 % is indicated which is promising. Though a promising potential exists, the results are strongly influenced by the ambient air temperature.

4.5. Limitations of the work

An attempt has been made in this work to explore the potential of free space cooling under real-time environmental conditions. However, long-term experimental investigations, economic analysis, and better-working prototypes may be developed to realize the full potential of this technology. The analysis can be extended to explore the following parameters:

- use of alternative PCM and encapsulation materials
- optimized heat exchanger design
- effect of placement (position) of the PCM
- effect of air flow rate on the melting and solidification time

Consideration of the above points can lead to better performance and optimization of the system in actual atmospheric conditions.

5. CONCLUSIONS

Integration of thermal energy storage into the building envelope has a promising potential for reducing energy footprint especially for space cooling applications. In this work, a novel design of an air-PCM heat

Global Digital Central
ISSN: 2151-8629

exchanger has been proposed, to provide a cooling effect of 1.25 TR comparable to a small apartment room. Night-time cool air is used to charge the PCM. Space cooling is achieved when hot room air is allowed to flow over the cold PCM in the said heat exchanger thus providing passive cooling. Experimental trials are carried out in actual climatic conditions to evaluate the potential for reduction in conventional air conditioner capacity. Numerical modelling of the system is done to predict the PCM temperature at discharge conditions. Investigations carried out for melting (discharge) in actual environmental conditions with 30 kg of PCM T25™ having melting point in the range of 24oC to 26oC were validated with a numerical model.

Experimental trials show that about 25% to 75 % of the PCM was solidified when subjected to cooling by cool air during the night-time with air temperature varying from 22 to 25oC. A solidification time of about 130 minutes was required when a relatively high air velocity of 17 m/s was maintained. Maximum solidification to the extent of 75% was registered under the aforesaid conditions. During discharge, the maximum temperature difference was 1.4oC and with an associated cooling effect of 2.05 kWth was obtained.

Air conditioner required for a 14 m^2 (150 ft^2) room can be downsized by using PCM based cooling system. The potential for reduction in A.C. capacity in the range of 13% to 46% depending on ambient temperature was ascertained. Free space cooling is an attractive proposition for regions having a diurnal temperature difference of the order of 12 to 14 K. Hence, this study is applicable to regions having similar diurnal temperature profiles.

Though with increase in the amount of solidified PCM, higher temperature drop was observed, use of PCM with a higher melting point is needs to be explored as it would assure complete solidification even if the night-time air temperature was greater during peak summer months. Alternative encapsulation techniques also need to be considered for quick as well as cost effective heat transfer surface. These are the areas for further investigation.

NOMENCLATURE

A	Area, m^2
c	Specific heat of melting, J/kg ^oC
k	Thermal conductivity, W/m K
f	fraction of liquid in the PCM
h	Heat transfer coefficient, W/m^2K
k	Thermal Conductivity W/ m KΔ
H	Enthalpy, kJ/kg
m	Mass, kg
$\dot{m}$	Mass flow rate, kg/s
N	Number of nodes
Nu	Nusselt Number
O	Number of cccupants in the room
q	Sensible heat of PCM, J/kg
Q	Heat transfer rate, kW
Re	Reynolds Number
Pr	Prandtl Number
T	Temperature, ^oC
t	Time, minutes
U	Overall heat transfer coefficient
V	Volume of infiltrated air, m^3
l	Length of the numerical computational domain
L	Latent heat of PCM, J/kg
x	Infinitesimal distance in x-direction
Δx	Thickness of the node
Δt	Differential thickness

Subscript

Inf	Infiltration
occ	Occupant
P	PCM
w	Wall

Greek

ρ	Density, kg/m^3
ω	Specific humidity

Abbreviations

AC	Air Conditioner
ACH	Air Changes per Hour
CLTD	Cooling Load Temperature Difference
CV	Control Volume
PCM	Phase Change Material
SC	Shading coefficient
SGHF	Solar Heat Gain Factor
TR	Tons of Refrigeration

REFERENCES

Al-mudhafar, A. H. N., Hamzah, M. T., & Tarish, A. L. , 2021, Potential of integrating PCMs in residential building envelope to reduce cooling energy consumption. Case Studies in Thermal Engineering, 27(July), 101360. https://doi.org/10.1016/j.csite.2021.101360

Arora, C. P., 2000, Refrigeration and Air Conditioning. Tata McGraw-Hill. https://books.google.co.in/books?id=JyGeRoZIy80C

Bohórquez-Órdenes, J., Tapia-Calderón, A., Vasco, D. A., Estuardo-Flores, O., & Haddad, A. N., 2021, Methodology to reduce cooling energy consumption by incorporating PCM envelopes: A case study of a dwelling in Chile. Building and Environment, 206(April). https://doi.org/10.1016/j.buildenv.2021.108373

Castell, A., Martorell, I., Medrano, M., Pérez, G., & Cabeza, L. F. , 2010, Experimental study of using PCM in brick constructive solutions for passive cooling. Energy and Buildings, 42(4), 534–540. https://doi.org/10.1016/j.enbuild.2009.10.022

De Gracia, A., & Cabeza, L. F. , 2015, Phase change materials and thermal energy storage for buildings. Energy and Buildings, 103, 414–419. https://doi.org/10.1016/j.enbuild.2015.06.007

Iten, M., Liu, S., & Shukla, A. , 2016, A review on the air-PCM-TES application for free cooling and heating in the buildings. Renewable and Sustainable Energy Reviews, 61, 175–186. https://doi.org/10.1016/j.rser.2016.03.007

ISHRAE Data-Book. 2017, Available from https://shop.ishrae.in/product/details/hvac-databook-/36

Khan, M., Ibrahim, M., & Saeed, T. , 2022, Space cooling achievement by using lower electricity in hot months through introducing PCM-enhanced buildings. Journal of Building Engineering, 53(April), 104506. https://doi.org/10.1016/j.jobe.2022.104506

Lazaro, A., Dolado, P., Marin, J. M., & Zalba, B. , 2009, PCM-air heat exchangers for free-cooling applications in buildings: Empirical model and application to design. Energy Conversion and Management, 50(3), 444–449. https://doi.org/10.1016/j.enconman.2008.11.009

Li, S., Sun, G., Zou, K., & Zhang, X. , 2016, Experimental research on the dynamic thermal performance of a novel triple-pane building window filled with PCM. Sustainable Cities and Society, 27, 15–22. https://doi.org/10.1016/j.scs.2016.08.014

Liu, Z., Yu, Z. (Jerry), Yang, T., Qin, D., Li, S., Zhang, G., Haghighat, F., & Joybari, M. M., 2018, A review on macro-encapsulated phase change material for building envelope applications. Building and Environment, 144, 281–294. https://doi.org/10.1016/j.buildenv.2018.08.030

Medved, S., & Arkar, C. , 2008, Correlation between the local climate and the free-cooling potential of latent heat storage. Energy and Buildings, 40(4), 429–437. https://doi.org/10.1016/j.enbuild.2007.03.011

Mehling, H., & Cabeza, L. F. , 2008, Solid-liquid phase change materials BT - Heat and cold storage with PCM: An up to date introduction into basics and applications (H. Mehling & L. F. Cabeza (eds.); pp. 11–55). Springer Berlin Heidelberg. https://doi.org/10.1007/978-3-540-68557-9_2

Moreno, P., Miró, L., Solé, A., Barreneche, C., Solé, C., Martorell, I., & Cabeza, L. F. , 2014, Corrosion of metal and metal alloy containers in contact with phase change materials (PCM) for potential heating and cooling applications. Applied Energy, 125, 238–245. https://doi.org/10.1016/j.apenergy.2014.03.022

Prabhakar, M., Saffari, M., de Gracia, A., & Cabeza, L. F., 2020, Improving the energy efficiency of passive PCM system using controlled natural ventilation. Energy and Buildings, 228, 110483. https://doi.org/10.1016/j.enbuild.2020.110483

Ramakrishnan, S., Wang, X., Alam, M., Sanjayan, J., & Wilson, J. , 2016, Parametric analysis for performance enhancement of phase change materials in naturally ventilated buildings. Energy and Buildings, 124, 35–45. https://doi.org/10.1016/j.enbuild.2016.04.065

Ratnakar Kulkarni, U. S. and P. C. , 2015, An Experimental Investigation of Free Space Cooling by Phase Change Material (PCM). International Journal of Engineering Technology and Sciences (Ijets), December, 4–10. https://doi.org/10.15282/ijets.4.2015.1.3.1032

Reyes-Cubas, A., & Abdo, P. , 2020, Simulation of Ventilation Flow at Different Conditions Through a Two-Dimensional Room Incorporated With Phase Change Materials. https://doi.org/10.1115/IMECE2020-23407

Ručevskis, S., Akishin, P., & Korjakins, A. , 2020, Parametric analysis and design optimisation of PCM thermal energy storage system for space cooling of buildings. Energy and Buildings, 224. https://doi.org/10.1016/j.enbuild.2020.110288

Song, M., Niu, F., Mao, N., Hu, Y., & Deng, S., 2018, Review on building energy performance improvement using phase change materials. Energy and Buildings, 158, 776–793. https://doi.org/10.1016/j.enbuild.2017.10.066

Sun, X., Zhang, Y., Xie, K., & Medina, M. A. , 2022, A parametric study on the thermal response of a building wall with a phase change material (PCM) layer for passive space cooling. Journal of Energy Storage, 47, 103548. https://doi.org/https://doi.org/10.1016/j.est.2021.103548

Turnpenny, J. R., Etheridge, D. W., & Reay, D. A. , 2000, Novel ventilation cooling system for reducing air conditioning in buildings. Part I: Testing and theoretical modelling. Applied Thermal Engineering, 20(11), 1019–1037. https://doi.org/10.1016/S1359-4311(99)00068-X

Waqas, A., & Kumar, S. , 2011, Utilization of latent heat storage unit for comfort ventilation of buildings in hot and dry climates. International Journal of Green Energy, 8(1), 1–24. https://doi.org/10.1080/15435075.2010.529406

Weinläder, H., Klinker, F., & Yasin, M. , 2016, PCM cooling ceilings in the Energy Efficiency Center - Passive cooling potential of two different system designs. Energy and Buildings, 119, 93–100. https://doi.org/10.1016/j.enbuild.2016.03.031